



## APPLICATION OF DIGITAL IMAGE CORRELATION TECHNIQUE TO TENSILE TEST FOR PRINTED PLA SPECIMENS

Murat AYDIN, Özkan ÖZ

Karabuk University, Technology Faculty, Industrial Design Engineering, Karabuk

### ABSTRACT

This study presents an approach to determine strain-stress curves of printed PLA material using 2D Digital Image Correlation (DIC) method. Besides, the present paper is an extended version of the previous study of the authors [1]. The tensile specimens were printed with a constant infill ratio and performed uniaxial tensile test with various test speeds. The elongations and local strains were measured with 2D DIC. Stress vs. strain curves were calculated from force data and DIC measurement. As a result, ultimate tensile stresses were directly proportional with the test speed increments, and maximum forces as well. The elongations were observed to decline during the test speed increments. It was underlined that the elongations gave the average results instead of the real behavior of the fractured area.

**KEYWORDS:** 3D Printer, PLA, Digital Image Correlation, Tensile Test, Strain, Stress.

### 1. INTRODUCTION

Digital Image Correlation (DIC) has drawn much attention recently due to obtain more information about the mechanical behavior of materials both plastics and metals. The fundamental of DIC depends on recording whole process as images, processing the images in terms of comparing undeformed image with deformed image sequence. By means of this comparison, the displacement and strain distribution can be obtained at sub-pixel level.

In the literature, there many studies were performed the application of DIC methods to material testing for both metal and non-metal materials, especially for plastic materials because of exhibiting inhomogeneous behavior and composites as well. Hild [2] and Roux presented a general overview of the digital image correlation to identify elastic properties from displacement measurement. Hung [3] and Voloshin presented a fast and simple (FAS) detection algorithm based on the digital image correlation for measurement of the surface deformation of planar objects. Their purposed fine search algorithm at pixel level resolution and surface fitting for sub-pixel level. They showed that the experimental data were in good agreement with the theoretical solution. Catalonatti [4] et al. studied on the identification of the crack tip location using digital image correlation and the calculation of the J-integral directly from the test data. They showed that the results obtained from DIC measurement and experiments exhibits similar to those obtained using finite element based methods for compact tension carbon–epoxy specimens. Wattrisse [5] et al. developed an imaging technique to study the strain localization phenomena that occur during the tension of thin, flat steel samples. They processed data using digital speckle image correlation to derive the two in-plane components of the displacement vectors. They proved that the accuracy was quite sufficient to track the inception and the development of localization. Périé [6] et al. focused on the identification of anisotropic damage law for composite material using digital image correlation and biaxial test. They used the DIC technique based on a finite element discretization to extract planar displacement fields and the reconditioned Equilibrium Gap Method to retrieve a damage law. They showed that the identified damage pattern and the corresponding damage values were similar to post-processed maps using classically identified parameters and the

reconstructed displacement field accounted for 95% of the fluctuations observed in the measurements. Klift [7] et al. focused on the printing of carbon fiber reinforced tensile test specimens using commercial 3D printer. They performed tensile test to compare experiment results with literature values for composite materials. They found out that discontinuities of the fibers cause to failures in the specific regions that lack of the fibers. Besides, they proved that elastic modulus of the 2CF and 6CF composites gave expected results. Sutradhar [8] et al. studied on the experimental validation of 3D printed patient-specific implants using digital image correlation and finite element analysis. They designed patient-specific bone replacement shapes using topology optimization and performed mechanical testing on a 3D printed bone replacement by applying masticatory forces. They validated the strains of the tests with digital image correlation and finite element analysis. As a result, they proved that the computational and experimental approach to designing patient-specific implants proved to be a viable technique for mid-face craniofacial reconstruction. Lee [9] et al. studied on measurement of anisotropic compressive strength of rapid prototyping parts. They used an ABS material for fused deposition modeling process, a zp102 (plaster powder) material for the 3D printer, and an acrylic-hydroxyapatite (40 wt%) composite material for nano-composite deposition system and performed compression test at 1.0mm/min loading rate according to ASTM D695. They found out that all the specimens exhibited anisotropic compressive properties. Besides, they showed that build direction was an essential printing parameter that had directly influence on the mechanical properties of printed parts. Meng [10] et al. studied to obtain 3D full-field deformation of a carbon fiber/epoxy composite pressure vessel using a 3D digital speckle correlation method. They evaluated the 3D full field displacement and strain distribution of the composite pressure vessel under internal pressure loading. They showed that the average strain value showed good agreement with the results obtained from conventional electrical-resistance strain gauge technology and the 3D digital speckle correlation method was suitable for deformation measurement of composite pressure vessels in real engineering practice. Grytten [11] et al. purposed an experimental investigation of the mechanical behavior of a talc and elastomer modified polypropylene compound subjected to large strains. They used 3D digital image correlation with two cameras and stereo-vision technique to determine full-field displacements during uniaxial tensile tests on specimens with rectangular cross-section. They showed that local strains can be derived from the displacement field. Giordano [12] et al. studied printing of polylactic acid structures using 3D printer and determining mechanical properties of printed parts as well. They manufactured test bars from low and high molecular weight PLA powders with chloroform used as a binder and applied cold isostatic pressing after printing process. They pointed out that maximum tensile strengths were measured as  $17.40 \pm 0.71$  MPa for the low molecular weight PLLA (53 000) and as  $15.94 \pm 1.50$  MPa for high molecular weight PLLA (312 000) as well. Tymrak [13] et al. studied on the basic tensile strength and elastic modulus of printed components using realistic environmental conditions for standard users of a selection of open-source 3-D printers. They determined the average tensile strengths as 28.5 MPa for ABS and 56.6 MPa for PLA with average elastic modulus of 1807 MPa for ABS and 3368 MPa for PLA. They pointed out that printed parts from tuned, low-cost, open-source RepRap 3D printers could be considered as mechanically functional in tensile applications as those from commercial vendors. Bellini [14] and Güçeri studied on fabrication of ceramic and multi-functional components using fused deposition modeling. They presented a methodology in order to characterize mechanical properties of produced parts using FDM. They performed tensile test using the dog-bone specimens and three-point bending tests as well. They proved that the mechanical properties of the final parts depended on the chosen building direction, the substrate, and chosen path.

## 2. MATERIAL AND METHOD

### 2.1. Material

In this study, uniaxial tensile test specimens were printed according to ASTM D638-10 [15] standard using 3D printer. PLA filament was used as printer material and infill ratio was set about 100% for each specimen. Figure 1 shows the dimensions of the tensile specimens. Zwick Roell 50kN test machine was used to perform experiments. Force and displacement values were obtained from test machine.

Tensile test specimens were modelled using SolidWorks software and 3D model was imported to the CURA software in order to print. 3D printer table temperature was set as 60°C and printing temperature

was about 200°C, as well. The thickness of part was 3mm. So, model was divided about 11 layers with Slic3r tool and layer height was set as 0.27mm. The printing speed was used as 70mm/s for all printing operations. Figure 2 shows the sliced and printed part in CURA software.

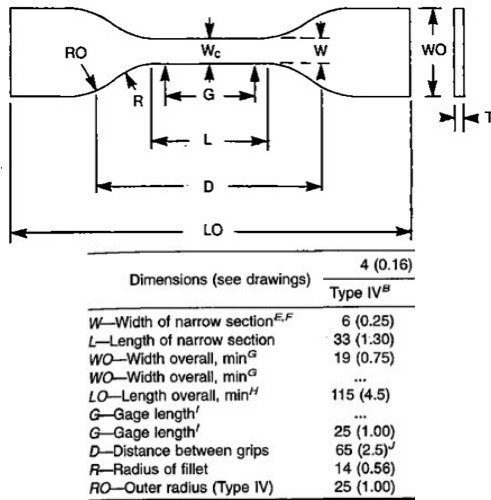


Figure 1. ASTM D638-10 Type IV specimen dimensions[7].

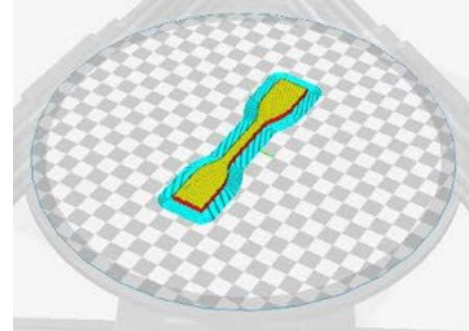


Figure 2. The printed part in CURA software

## 2.2. Method

In the experiments, 2D DIC method was used to measure elongation and distributions of displacement and strain instead of traditional extensometer. In 2D DIC method, the high-resolution camera is mounted to the perpendicular position to the object surface and recorded whole deformation process. By means of using high resolution and high frame per second (fps) camera, the accuracy and precision of the measurement is increased gradually. In this study, Canon T3i DSLR camera was used with a 58mm diameter and 18-55mm (f/3.5-5.6) macro lens. All the experiments were recorded with 1280x720 pixels resolution and 60fps. Figure 3 shows the schematic view of installed 2D DIC measurement setup.

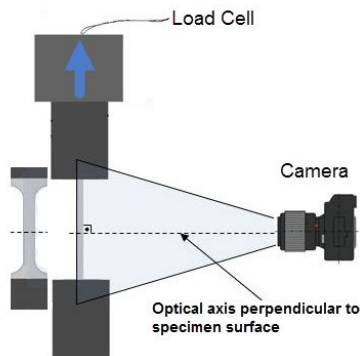


Figure 3. The schematic view of 2D DIC measurement.

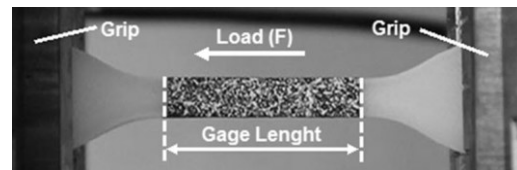


Figure 4. Painted specimen with the gage length

In order to get high and accurate correlation, random spackle pattern must be small enough and dense. In this study, acrylic matt white and black spray paints were used to create background and speckles onto specimen surface. In the first step, matt black paint was applied for background and then matt white spackles were created on this background. In 2D DIC, calibration is needed in order to convert pixel values to the known units, such as “m” or “mm”. Besides, gage length in ASTM D638-10 was specified as 25mm that is the proper space for measurement. Therefore, on the specimen surface, the window which was included gage length area was created by two Scott types that shielded the paint. After the paint was dried, the types were peeled out, leaving clear boundary of the tensile gage length. Figure 4 shows the painted specimen with the gage length. Laboratory lighting condition was enough to have clear view, so extra lightning source was not needed.

### 3. EXPERIMENTAL RESULTS

Uniaxial tensile tests were performed for each specimen using three different test speeds, 1mm/s, 0.1mm/s, and 0.05mm/s. Force and displacement values were obtained from tensile machine. The maximum forces were 615.80N and 565.12N using 0.05mm/s test speed for Specimen No.1, No.2 respectively. On the other hand, maximum forces were obtained using 0.1mm/s test speed for each specimen as 661.14N and 655.61N respectively. In addition, when the test speed was increased to 1mm/s, the maximum forces were measured as 732.11N and 688.44N for each specimen respectively. It was shown that when the test speed increased, the maximum forces were increased relatively.

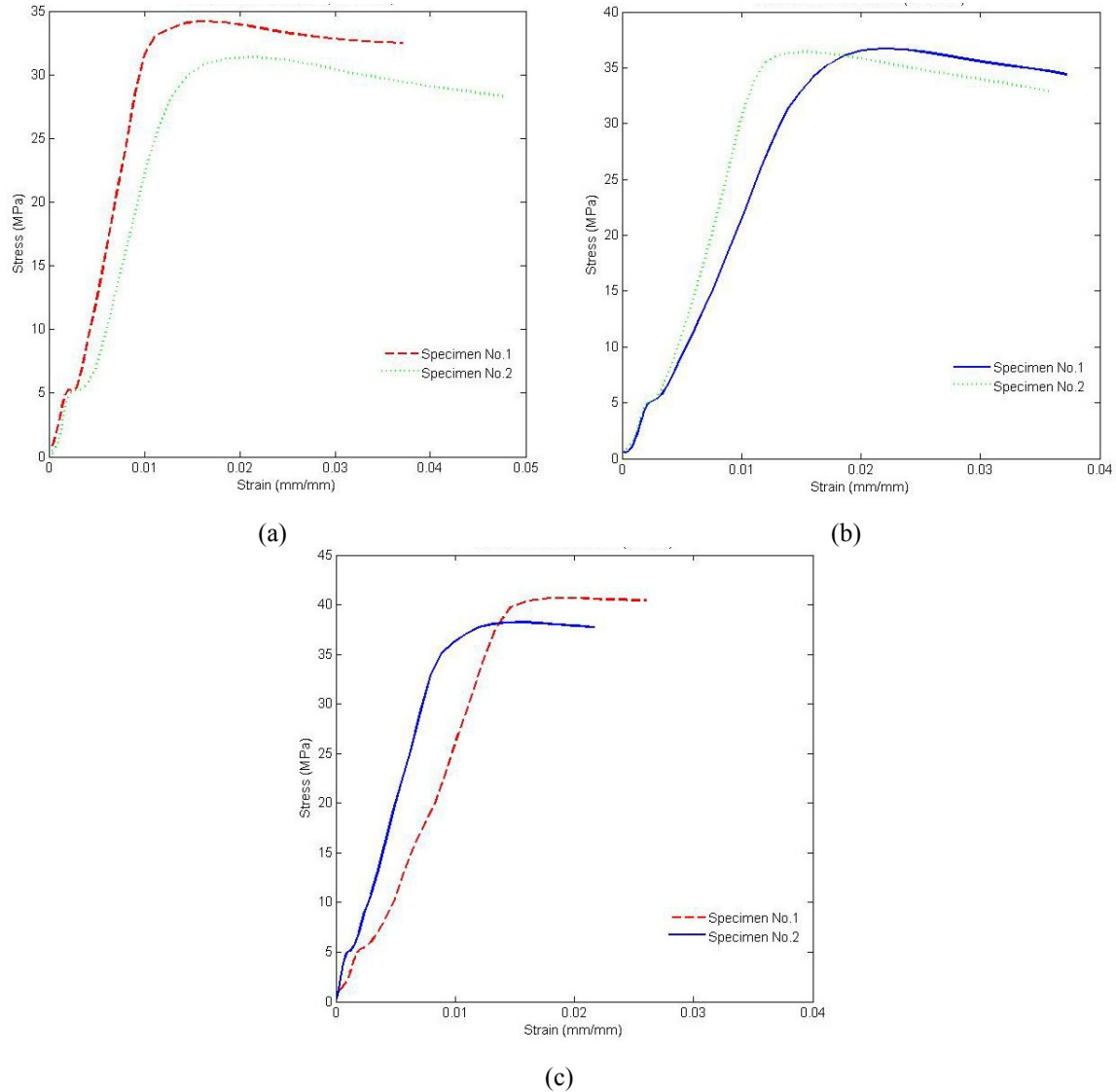


Figure 5. The strain vs. stress curves for (a)0.05mm/s, (b)0.1mm/s, (c)1mm/s test speeds.

For the calculation of non-contact measurement, the virtual extensometer from DIC system using the images covering the same gage length. The extension was created from the images using VIC-2D software. Using force data, the stress values were calculated by dividing force value to cross sectional area. Figure 5 shows the measured strain values vs. calculated stress values of two specimens for each test speed. The ultimate tensile stresses were calculated as 34.21MPa and 31.39MPa using Specimen No.1 and Specimen No.2 for 0.05mm/s test speed respectively. When the test speed was increased to 0.1mm/s, the ultimate tensile stresses were calculated as 36.73MPa and 36.42MPa for Specimen No.1 and Specimen No.2 respectively. In addition, using 1mm/s test speed that was the highest speed in experiments, the ultimate tensile stresses were calculated as 40.67MPa and 38.24MPa for Specimen No.1 and Specimen No.2 respectively. The maximum ultimate tensile stress values were obtained using

highest test speed, 0.1mm/s. When the elongations were considered, the minimum elongations were measured using 1mm/s test speed as 0.026 and 0.021 for Specimen No.1 and No.2 respectively. Besides, the strain values of Specimen No.1 and No.2 were measured as 0.037 and 0.035 for 0.1mm/s test speed, and measured as 0.037 and 0.047 for 0.05mm/s test speed respectively. It was observed that the strain was greatly decreased when the test speed was increased to 1mm/s and there was a slightly differences between 0.05mm/s and 0.1mm/s test speeds.

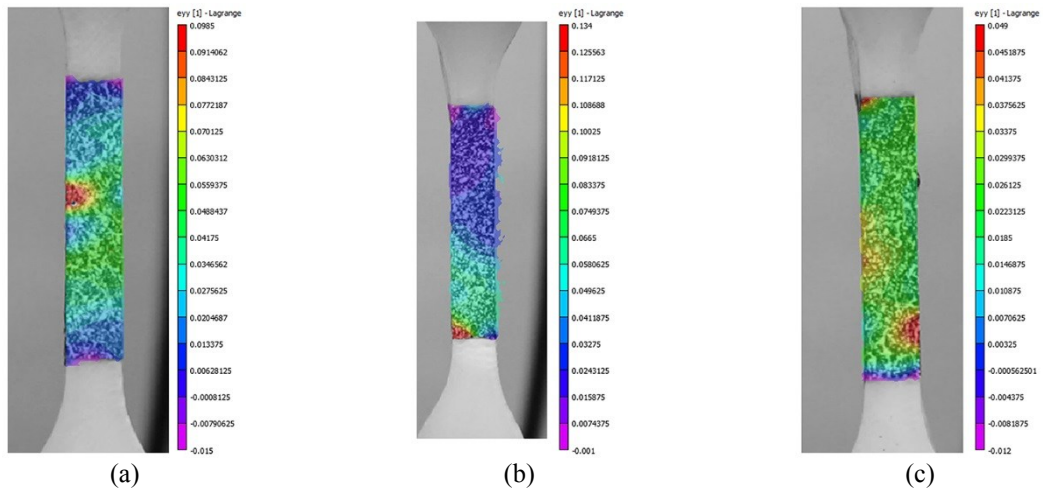


Figure 6. Strain distribution at y direction of Specimen No.1 for (a)0.05mm/s, (b)0.1mm/s, (c)1mm/s test speeds.

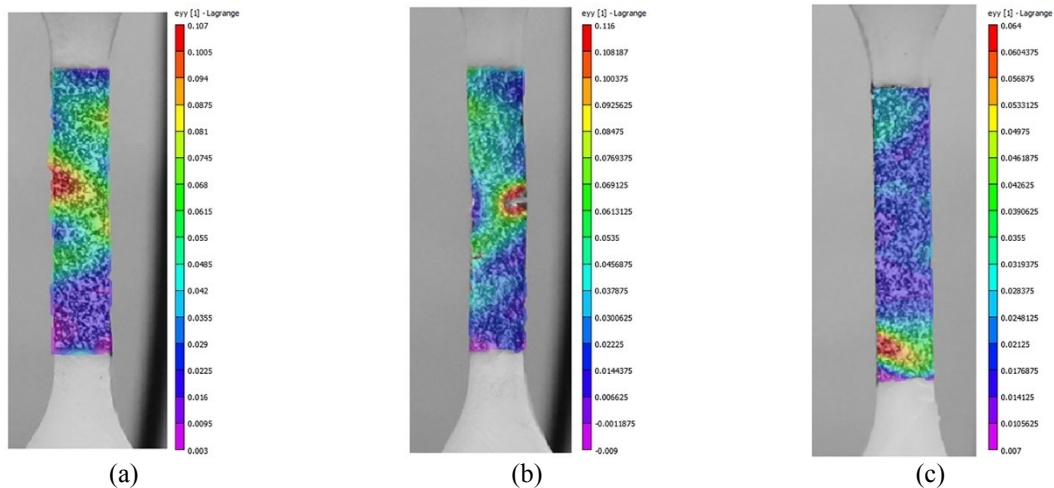


Figure 7. Strain distribution at y direction of Specimen No.2 for (a)0.05mm/s, (b)0.1mm/s, (c)1mm/s test speeds.

The most important feature of the DIC method is to measure full-field strain and displacement maps on entire surface of the specimen. Figure 6 and Figure 7 show the strain distributions in y direction which is the stretching direction of Specimen No.1 and Specimen No.2 for all test speeds, respectively. As seen in Figure 6 and Figure 7, strains at y direction can be presented as color scale bar from minimum to maximum strain values and images indicates at moment which is previous of the fracture in experiments. The red regions which are in the gage length expresses the maximum value of y direction strains where the deformation was localized. For those experiments, the maximum localized strain values before fracture were measured as 0.0985, 0.134, 0.049 for 0.05mm/s, 0.1mm/s, and 1mm/s test speeds for Specimen No.1, respectively (Figure 6). Besides, the maximum localized strain values were as 0.107, 0.116, 0.064 for same test speeds for Specimen No.2 (Figure 7). When the localized deformation compared with uniform deformation, it was shown that elongations were the average values in terms of mechanical behaviors of test specimens. However, localized strains were higher than the virtual extensometer approach values. In addition, similar to the elongation behavior, the local strain

was minimum value at highest test speed. On the other hand, the local strains for 0.05mm/s and 0.1mm/s test speeds were slightly increased.

#### 4. CONCLUSION

In this study, the tensile specimens which had %100 infill ratios were printed using 3D printer and performed to uniaxial tensile test with various strain rates in order to determine stress vs. strain curves and local strains using 2D digital image correlation technique. As a result;

- It was shown that the test speed had influence on the increasing maximum forces significantly.
- The average ultimate tensile stresses were calculated as 32.8MPa, 36.575MPa, 39.455MPa for 0.05mm/s, 0.1mm/s, and 1mm/s respectively. It was seen that the average tensile stresses varied from 32 MPa to 39MPa which was the similar value in previous studies [16,17] without considering printing orientation. Besides, it was shown that the average ultimate tensile stresses were raised depend on the increment of the test speed.
- The average strain was calculated as 0.042, 0.036, 0.023 for 0.05mm/s, 0.1mm/s, and 1mm/s respectively. It was seen that the average strains for 0.05mm/s and 0.1mm/s were similar to standard PLA elongation about 4% [18]. Besides, it was underlined that the average strains were decreased noticeably when the test speed was increased.
- In terms of localized strains, it was pointed out that the maximum localized strains at y direction always were higher than the virtual extensometer approach and for those experiments, fracture points always locate in the higher strains regions at y direction.
- It was pointed out that the inhomogeneous printing was caused the differences between Specimen No.1 and Specimen No.2 in terms of strain-stress curves because of the fact that print orientation, infill, shells, material age, and slicer operations effect the mechanical properties of material [19].
- It was determined that the digital image correlation technique was a useful, easy measurement method at least for this type of material and this type of experiment setup [11].

#### REFERENCES

- [1]. Aydin M and Öz Ö. Determination of Mechanical Behaviour of Printed PLA Specimens Using Digital Image Correlation. International Symposium on Industry 4.0 and Applications (ISIA 2017). 2017.
- [2]. Hild F, Roux S. Digital Image Correlation: from Displacement Measurement to Identification of Elastic Properties – a Review. *Strain*. 2006; 42(2): 69-80.
- [3]. Po-Chih H, Voloshin AS. In-plane strain measurement by digital image correlation. *Journal of the Brazilian Society of Mechanical Sciences and Engineering*. 2003; 25(3).
- [4]. Catalanotti G, Camanho PP, Xavier J, Dávila CG, Marques AT. Measurement of resistance curves in the longitudinal failure of composites using digital image correlation. *Composites Science and Technology*. 2010; 70(13): 1986-1993.
- [5]. Watrisse B, Chrysochoos A, Muracciole JM, Némoy-Gaillard M. Analysis of strain localization during tensile tests by digital image correlation. *Experimental Mechanics*. 2001; 41(1): 29–39.
- [6]. Jean NP, Hugo L, Stéphane R, François H. Digital image correlation and biaxial test on composite material for anisotropic damage law identification. *International Journal of Solids and Structures*. 2009; 46(11–12): 2388-2396.
- [7]. Klift FVD, Koga Y, Todoroki A, Ueda M, Hirano Y, Matsuzaki R. 3D Printing of Continuous Carbon Fibre Reinforced Thermo-Plastic (CFRTP) Tensile Test Specimens. *Open Journal of Composite Materials*. 2016; 6: 18-27.
- [8]. Sutradhar A, Park J, Carrau D, Miller MJ. Experimental validation of 3D printed patient-specific implants using digital image correlation and finite element analysis. *Computers in Biology and Medicine*. 2014; 52: 8-17.
- [9]. Lee CS, Kim SG, Kim HJ, Ahn SH. Measurement of anisotropic compressive strength of rapid prototyping parts. *Journal of Materials Processing Technology*. 2007;187-188: 627-630.
- [10]. Meng LB, Jin GC, Yao XF, Yeh HY. 3D full-field deformation monitoring of fiber composite pressure vessel using 3D digital speckle correlation method. *Polymer Testing*. 2006; 25(1): 42-48.

- [11]. Grytten F, Daiyan H, Polanco-Loria M, Dumoulin S. Use of digital image correlation to measure large-strain tensile properties of ductile thermoplastics. *Polymer Testing*. 2009; 28(6): 653-660.
- [12]. Russell AG, Benjamin MW, Scott WB, Linda GC, Emanuel MS, Michael JC. Mechanical properties of dense polylactic acid structures fabricated by three-dimensional printing. *Journal of Biomaterials Science, Polymer Edition*. 1997; 8(1): 63-75.
- [13]. Tymrak BM, Kreiger M, Pearce JM. Mechanical properties of components fabricated with open-source 3-D printers under realistic environmental conditions. *Materials and Design*. 2014; 58: 242-246.
- [14]. Bellini A and Güçeri S. Mechanical characterization of parts fabricated using fused deposition modeling. *Rapid Prototyping Journal*. 2003; 9(4): 252–264.
- [15]. ASTM D638-10. Standard Test Method for Tensile Properties of Plastics. ASTM International. West Conshohocken, PA, 2010, [www.astm.org](http://www.astm.org)
- [16]. Malik R. Tensile Testing of 3D Printed Materials for Scoliosis Brace (Master's Thesis). India. 2017.
- [17]. Kim H, Park E, Kim S, Park B, Kim N, Lee S. Experimental Study on Mechanical Properties of Single- and Dual-Material 3D Printed Products. *Procedia Manufacturing*. 2017; 10: 887–897.
- [18]. PLA Technical Data Sheet. SD3D. 2017; [https://www.sd3d.com/wp-content/uploads/2017/06/MaterialTDS-PLA\\_01.pdf](https://www.sd3d.com/wp-content/uploads/2017/06/MaterialTDS-PLA_01.pdf)
- [19]. PLA and ABS Strength Data. Makerbot. 2017; [http://download.makerbot.com/legal/MakerBot\\_R\\_PLA\\_and\\_ABS\\_Strength\\_Data.pdf](http://download.makerbot.com/legal/MakerBot_R_PLA_and_ABS_Strength_Data.pdf)